AD-A110 818 NAVAL POSTGRADUATE SCHOOL MONTEREY CA F/G 20/6
DISTRIBUTED APERTURES IN LAMINAR FLOW LASER TURRETS.(U)
SEP 81 B B TOUSLEY
UNCLASSIFIED NPS-67-81-014 NL

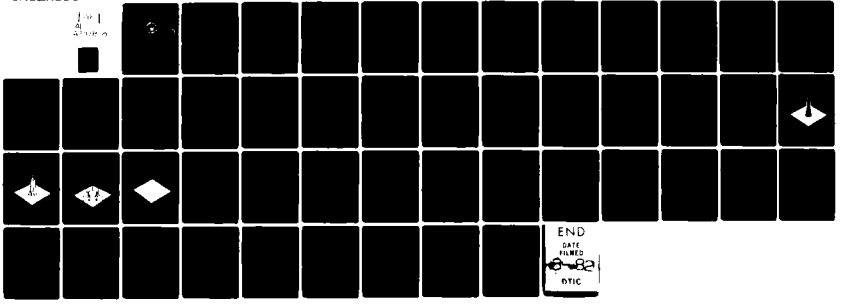

END
DATE FILMED
6-82
DTIC

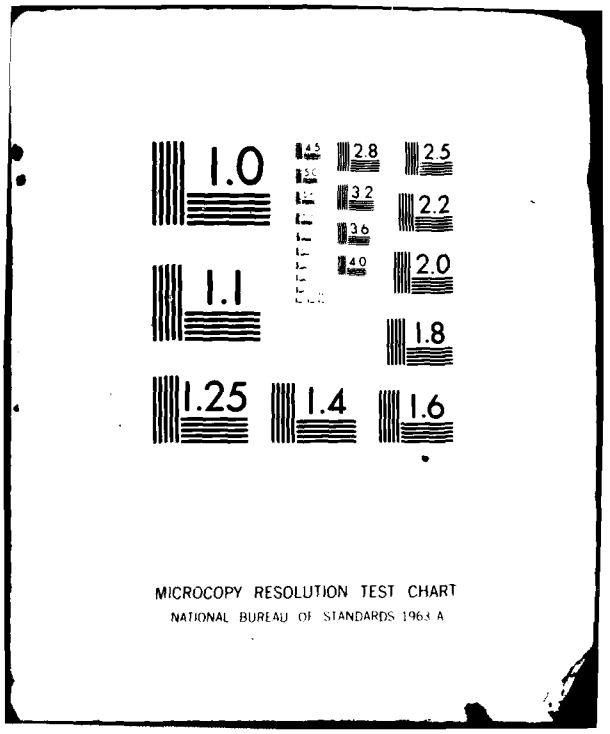
1.0
1.1
1.25
1.4
1.6
1.8
2.0
2.2
2.5
2.8
3.2
3.6
4.0
MICROCOPY RESOLUTION TEST CHART
NATIONAL BUREAU OF STANDARDS 1963 A

NPS 67-81-014

NAVAL POSTGRADUATE SCHOOL

Monterey, California

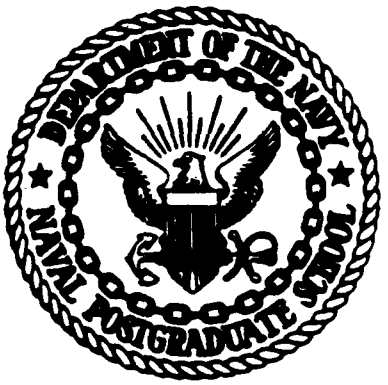

THESIS

Distributed Apertures in Laminar Flow Laser Turrets

by

Brian Brooks Tousley

September 1981

Thesis Advisor: Allen E. Fuhs

Approved for public release; distribution unlimited

Prepared for:

Air Force Weapons Laboratory/ARLB
Kirtland AFB, New Mexico 87117

UNCLASSIFIED

SECURITY CLASSIFICATION OF THIS PAGE (When Data Entered)

REPORT DOCUMENTATION PAGE		READ INSTRUCTIONS BEFORE COMPLETING FORM
1. REPORT NUMBER NPS 67-81-014	2. GOVT ACCESSION NO. AD-A110 818	3. RECIPIENT'S CATALOG NUMBER
4. TITLE (and Subtitle) Distributed Apertures in Laminar Flow Laser Turrets		5. TYPE OF REPORT & PERIOD COVERED Masters Thesis/Technical Report - September 1981 6. PERFORMING ORG. REPORT NUMBER
7. AUTHOR(s) Brian Brooks Tousley		8. CONTRACT OR GRANT NUMBER(s) 80-MP-084
9. PERFORMING ORGANIZATION NAME AND ADDRESS Naval Postgraduate School Monterey, California 93940		10. PROGRAM ELEMENT, PROJECT, TASK AREA & WORK UNIT NUMBERS 81-MP-071
11. CONTROLLING OFFICE NAME AND ADDRESS AFWL/ARLB Kirtland AFB, NM 87117		12. REPORT DATE September 1981 13. NUMBER OF PAGES
14. MONITORING AGENCY NAME & ADDRESS(if different from Controlling Office)		15. SECURITY CLASS. (of this report) Unclassified 15a. DECLASSIFICATION/DOWNGRADING SCHEDULE

16. DISTRIBUTION STATEMENT (of this Report)

Approved for public release; distribution unlimited.

17. DISTRIBUTION STATEMENT (of the abstract entered in Block 20, if different from Report)

18. SUPPLEMENTARY NOTES

19. KEY WORDS (Continue on reverse side if necessary and identify by block number)

High Energy Lasers
Aperture Arrays
Laser Turrets
Aero-Optics

20. ABSTRACT (Continue on reverse side if necessary and identify by block number)

Assume a technology that permits undistorted laser beam propagation from the aft section of a streamlined turret. A comparison of power on a distant airborne target is made between a single aperture in a large scale streamlined turret with a turbulent boundary layer and various arrays of apertures in small scale streamlined turrets with laminar flow. The array performance is mainly limited by the size of each aperture. From an array - (contd)

DD FORM 1 JAN 73 1473 EDITION OF 1 NOV 65 IS OBSOLETE
S/N 0102-014-6601

UNCLASSIFIED
SECURITY CLASSIFICATION OF THIS PAGE (When Data Entered)

Item 20. (Contd.)

one might expect, at best, about 40 percent as much power on the target as from a single aperture with equal area. Since the turbulent boundary layer on the large single-turret has negligible effect on beam quality, the array would be preferred (if all development efforts were essentially equal) only if a laminar wake is an operational requirement.

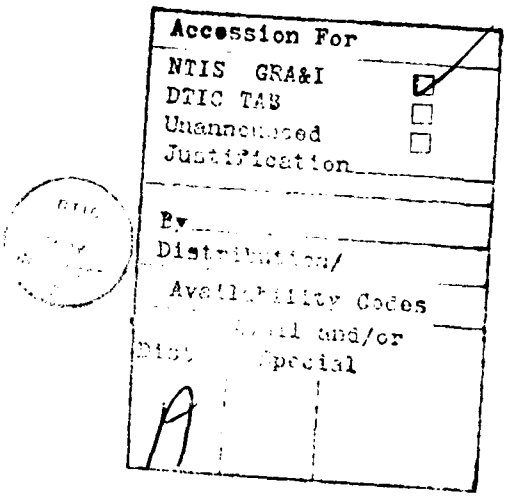

Approved for public release, distribution unlimited

Distributed Apertures in Laminar Flow Laser Turrets

by

Brian Brooks Tousley
Lieutenant, United States Coast Guard
B.S., United States Coast Guard Academy, 1976

Submitted in partial fulfillment of the
requirements for the degree of

MASTER OF SCIENCE IN PHYSICS

from the

NAVAL POSTGRADUATE SCHOOL
September 1981

Author: Brian B Tousley

Approved by: Allen E Fuhs
Thesis Advisor

Second Reader

Chairman, Department of Physics and Chemistry

Dean of Science and Engineering

ABSTRACT

Assume a technology that permits undistorted laser beam propagation from the aft section of a streamlined turret. A comparison of power on a distant airborne target is made between a single aperture in a large scale streamlined turret with a turbulent boundary layer and various arrays of apertures in small scale streamlined turrets with laminar flow. The array performance is mainly limited by the size of each aperture. From an array one might expect, at best, about 40 percent as much power on the target as from a single aperture with equal area. Since the turbulent boundary layer on the large single-turret has negligible effect on beam quality, the array would be preferred (if all development efforts were esentially equal) only if a laminar wake is an operational requirement.

TABLE OF CONTENTS

LIST OF TABLES

LIST OF FIGURES

LIST OF SYMBOLS

a	energy containing turbulence wavelength, m
ΔA	incremental area element in the target plane, m^2
A	the area within "the Bucket", m^2
B	area of an aperture, m^2
C_1	constant of proportionality, watts m^{-2}
C_2	constant of proportionality, $m^{0.2}$
C_L	lift coefficient
d	interaperture spacing, m
D_s	single turret aperture diameter, m
D_A	individual aperture diameter in the array, m
F	array factor
h	altitude, km
H	scale height, km
I	irradiance on the target, watts m^{-2}
I_o	irradiance on axis on the target for a single aperture, watts m^{-2}
I_1	aperture factor
I_2	radiant emittance of the aperture, watts m^{-2}
I_{ij}	irradiance at a point in the target plane at grid coordinates i, j, watts m^{-2}
J_1	Bessel function of first order
k	wavenumber, m^{-1}
L	aerodynamic lift force, lbf; boundary layer thickness, m

L_A	maximum array dimensions, m
M	the number of grid points within "the Bucket"; Mach number
N	the number of apertures in an array
P_p	power projected, watts
R	perpendicular distance between aperture and target planes, m
R	Reynolds number
S	wing surface area, ft^2
T	temperature, K
T_o	stagnation temperature, K
V	flight velocity, m sec^{-1} and knots
X	distance from leading edge of flat plate, m
α	extinction coefficient for coherent beam in the turbulent boundary layer, m^{-1}
γ	ratio of heat capacities
$\Delta_2^{(j)}$	geometric path difference between a distance extending from a point in the target plane to a reference position in the j^{th} aperture, and the distance R, m
θ	angular divergence from beam axis
K	proportionality constant which relates refractive index to air density
λ	radiation wavelength, m
Λ	turbulence integral scale, m
ν	kinematic viscosity, m^2 sec
μ	dynamic viscosity, kg m^{-1} sec^{-1}
ρ	atmospheric density, kg m^{-3}
$\Delta\rho$	local change in density, kg m^{-3}

SUBSCRIPTS

A	array
c	critical
m	minimum
s	single
SL	sea level
w	wall or surface
∞	ambient

ACKNOWLEDGEMENTS

The author recognizes the unique opportunity to work under the tutelage of a man with the rare composite personal qualities of patience, kindness, an affinity for work and a vast technical ability.

The author also wishes to express his continuing appreciation to Mom and Dad for their love and resolve which encourages the author to fulfill his potential.

I. INTRODUCTION

Propagation of laser energy from an aircraft turret designed with today's technology to an airborne target is unacceptably degraded when the target is in the quadrant between 120° - 240° relative bearing due to the turbulent boundary layer and separated flow on the aft section of the turret. For Surface to Air Missile (SAM) defense, this is an especially interesting problem since the most dangerous threat to an aircraft is likely to approach from behind. Figure 1a is a diagram of such a turret. The fairing is needed to curtail heavy oscillatory aerodynamic loading.

Were the flow around such a turret laminar, an undispersed beam could be projected into the volume which the separated flow presently inhibits. Reduction of turret scale could - if sufficient - result in laminar flow. However, at aircraft flight velocities and turret scales of practical size, a separated flow region will exist in any case (Fig. 1b).

A future development may permit undistorted beam propagation from a window on the aft section of a streamlined body. In this event, a similar, though less severe beam degradation problem would probably still exist on the large scale due to the turbulent boundary layer (Fig. 1c). Note

the large scale turret would have a turbulent wake. A laser beam propagated through the turbulent wake would be severly degraded.

The small scale streamlined body however, could achieve laminar flow (Fig. 1d). Such a body with a future technology window could project a beam without degradation from separated regions or turbulent boundary layers. Beam dispersion in a laminar wake is not significant. Reduction of body size would however require more apertures to project an amount of power equivalent to that from a single larger aperture. An array of many such small turrets in laminar flows with total aperture area equal to the area of the single aperture may be distributed around the aircraft away from aircraft turbulent wakes. If properly configured, such an array will achieve greater power on a target aft of the aircraft than any other of today's technology turret designs, and perhaps greater power on a target than the tomorrow's technology single-turret design. Henceforth, discussion is limited to laser turrets designed using this future "window" technology.

TODAY'S TECHNOLOGY (blunt base bodies on fuselage)

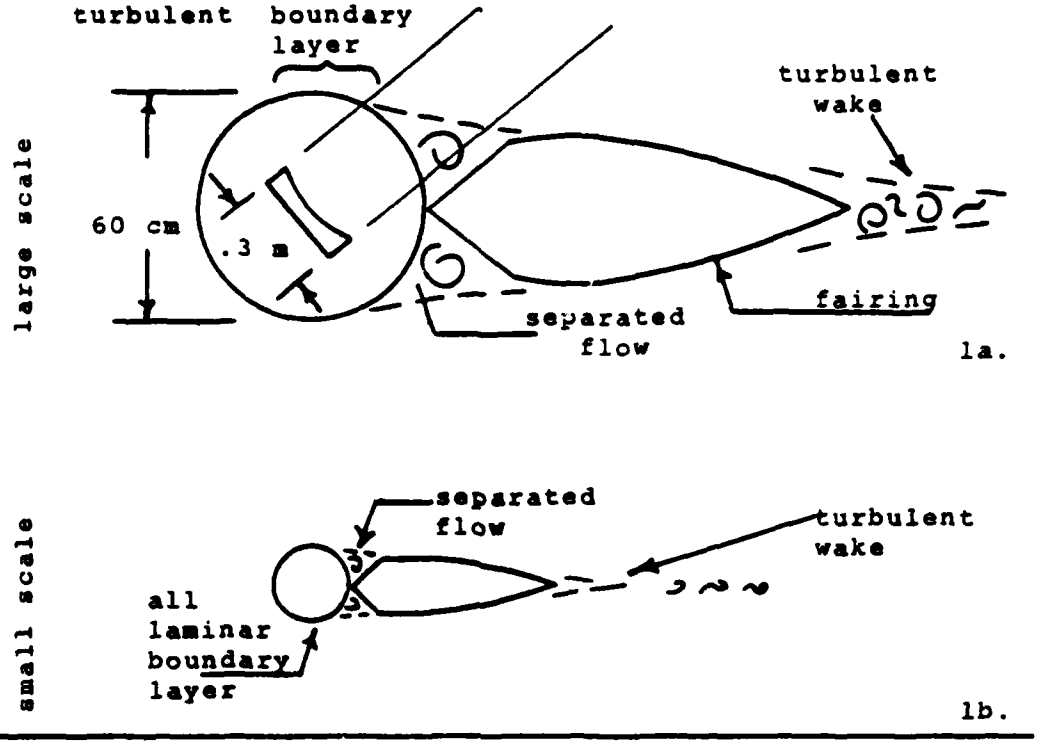

FUTURE TECHNOLOGY (streamlined bodies isolated from fuselage)

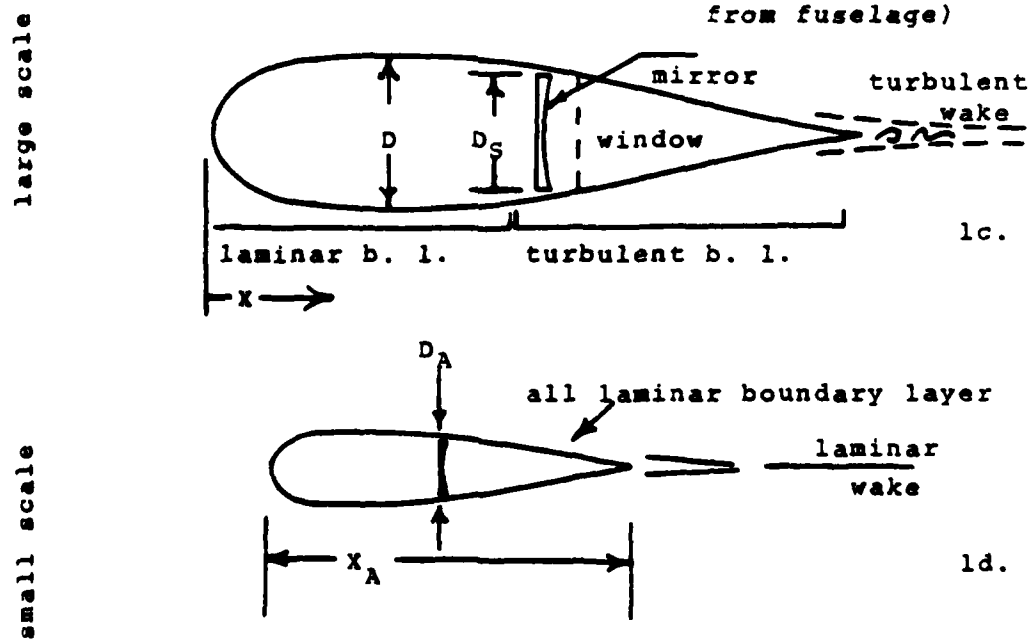

Fig. 1: PRESENT AND FUTURE TECHNOLOGY TURRET DESIGNS

II. METHOD

One seeks a quantitative comparison between the performance of the single larger aperture projecting a beam through a turbulent medium and an array of small apertures projecting beams through laminar flows which converge on a distant airborne target. For identification, the Single Aperture projecting through a Turbulent boundary layer will be SAT; the Array of apertures projecting through Laminar flows will be AL.

Isolation of the effects of the turbulent boundary layer on the single aperture and of the performance of the array in laminar flows is required to determine if greater power on the target can be achieved by the array. To do so requires the following assumptions:

1. No power losses in the atmosphere.
2. No thermal blooming effects.
3. No jitter.
4. A perfect pointer/tracker.

A reference area is defined as that area contained by the first zero of irradiance of the Airy disk which would be produced on the target in vacuo by the single aperture. This reference area is chosen believing that a single aperture design delivers sufficient destructive energy to a

target when projecting through a laminar flow and that energy outside of this area will not contribute to target destruction or will be insufficient to disable it. This reference area will be called "the Bucket".

Power in the Bucket (PIB) for the SAT and the AL will be compared. If the PIB for the array is found to be greater than that for the SAT, then the array would perhaps be more effective against targets approaching an aircraft from behind.

III. DIFFRACTION OF LASER BEAMS

The distribution of monochromatic (laser) irradiance on a target is - among other things - the result of diffraction.

A. SINGLE APERTURE

For the single circular aperture in the Fraunhofer region without any dispersive atmospheric effects the resultant distribution of irradiance is the well known Airy disk. Calculations show that 83.8% of the incident power arrives within the area contained by the first zero of the Airy distribution [Ref. 1].

B. ARRAY OF APERTURES

The array possesses maximum dimensions which are larger than the single aperture. Thus, the Fraunhofer condition may not be satisfied for the array at a target distance where it is satisfied for the single large aperture.

Figure 2 shows an array of apertures where O_1 is the source plane, O is the aperture plane, and O_2 is the target plane.

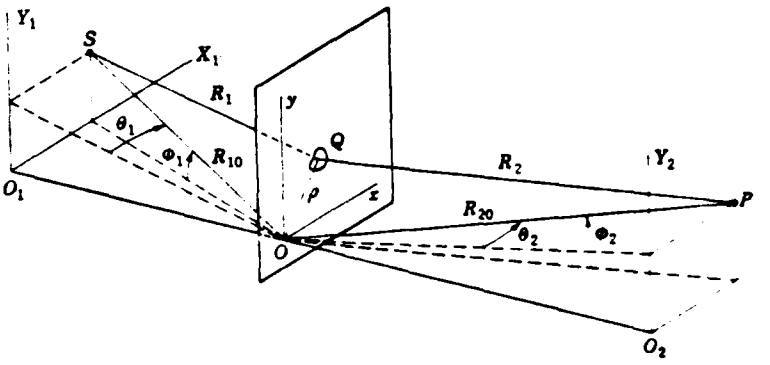

Fig. 2: COORDINATE SYSTEM FOR AN ARRAY DIFRACTION PROBLEM. REPRODUCED FROM STONE. [REF. 2]

For a plane wave incident on the aperture plane the Fraunhofer condition is satisfied when the maximum dimension of the array creates a phase difference less than 0.1λ in the target plane. This occurs when either of the following conditions are met.

1. The beam is collimated, and $L_A^2/R\lambda << 1$.
2. The array is focused at the target plane.

A lens has the effect of bringing the Fraunhofer region closer to the aperture plane. It does this by lengthening the geometric path length of light passing through the central part of the lens such that the Fraunhofer condition is satisfied near the focal point of the lens. Phase retardation across the aperture plane will have the same effect. This retardation can hopefully be accomplished by adaptive optics so that targets at close distances will be in the Fraunhofer region.

For simulation on a computer however, it is much easier to chose $R>>L_A^2/\lambda$ than to insert phase retardation across the apertures.

C. IRRADIANCE ON A TARGET FROM AN ARRAY OF APERTURES

The irradiance in the target plane is

$$I = C_1 I_1 F \tag{1}$$

where I_1 is the aperture factor, F is the array factor, and C_1 is a constant of proportionality. I_1 is a function of aperture size and shape, distance to and location on the target, and the wavelength. For identical circular apertures

$$I_1 = \left[\frac{2\,J_1(\sigma\pi)}{\sigma\pi}\right]^2 \tag{2}$$

where

$$\sigma = \frac{\Theta D_A}{\lambda} \tag{3}$$

F, the array factor, is the product [Ref. 3] of the conjugates of the sum of the complex phases at each point. The phases involved are a function of the array geometry, distance to and location on the target, and the wavelength.

$$F = \left| \sum_j^N e^{ik\Delta_2^{(j)}} \right|^2 \tag{4}$$

where

$$\Delta_2^{(j)} = -x\sin\Theta_2 - y\sin\phi_2 \tag{5}$$

Refer to Figure 2 for the geometry and definition of Θ_2 and ϕ_2. C_1 is chosen so that the irradiance on axis in the target plane is N^2 and has the units of watts/m^2. Substituting (2) and (4) into (1), the irradiance becomes

$$I = C_1 \left[\frac{2 J_1(\sigma\pi)}{\sigma\pi}\right]^2 \left| \sum_j^N e^{ik\Delta_2^{(j)}} \right|^2 \qquad (6)$$

To visualize the distribution of irradiance at the target and to calculate PIB, a grid of points (X_{2i}, Y_{2j}) is created in the target plane (see Fig. 2). At each point the phases and the argument of J_1 are computed. This yields I_{ij} at that point; I_{ij} is stored in an array. Those grid points within "the Bucket" contribute to the summation of PIB in the following manner:

The PIB for a continuous intensity distribution would be

$$PIB_{AL} = \iint_{\text{bucket}} I(x,y)\, dxdy \qquad (7)$$

This is approximated numerically as

$$PIB_{AL} = \sum_i^{\text{bucket radius}} \sum_j I_{ij}\, \Delta A \qquad (8)$$

which becomes

$$PIB_{AL} = \frac{A}{M} \sum_i^{\text{bucket radius}} \sum_j I_{ij} \qquad (9)$$

if the following further approximation is made:

$$\Delta A = \frac{A}{M} \tag{10}$$

This approximation of ΔA improves as the density of points in the grid becomes greater. Calculation of PIB for the Airy disk by this method with about 80,000 points in the bucket yields 83.5% of the total Power Projected (P_p) in the bucket. The published value is 83.8%. The program is in Appendix A.

The PIB obtained from Equation (9) is compared to the total power projected by the array to find the Fractional Power in the Bucket (FPIB). FPIB is the true measure of the "goodness" of a system of one or more apertures.

$$FPIB_{AL} = \frac{PIB_{AL}}{P_p} \tag{11}$$

Power projected is found by use of the relation for the on axis intensity from a single circular aperture.

$$I_o = I_2 \left[\frac{B_s}{\lambda R}\right]^2 \tag{12}$$

where I_2 is the intensity of the field in the aperture, B is the aperture area, λ is the wavelength, and R is the distance to the target from the aperture(s). So that for an array

$$I_o = I_2 \left[\frac{NB_A}{\lambda R}\right]^2 \tag{13}$$

The total power projected by the array is

$$P_p = I_2 \, NB_A \tag{14}$$

Radio astronomers use arrays of antennas; several papers [Refs. 4, 5] on radio astronomy were examined for concepts. Further, insects have eyes which contain a large number of elements in an array. The principals of insect vision [Refs. 6, 7] were also investigated.

The irradiance on the target plane was calculated for several array configurations; conditions for Fraunhofer diffraction existed. Figure 3 shows the FPIB achieved by each configuration. The best FPIB achieved for a 10-cm aperture was 48%.

For arrays in the triangular configuration (probable candidate for use on aircraft) with array aperture area equal to the area of the single aperture, the ratio D_A/D_s will also determine FPIB. Figure 5 shows this trend which is very insensitive to interaperture spacing so long as the Fraunhofer condition is satisfied; the behavior is true in general for all array configurations and is qualitatively apparent from Figure 4.

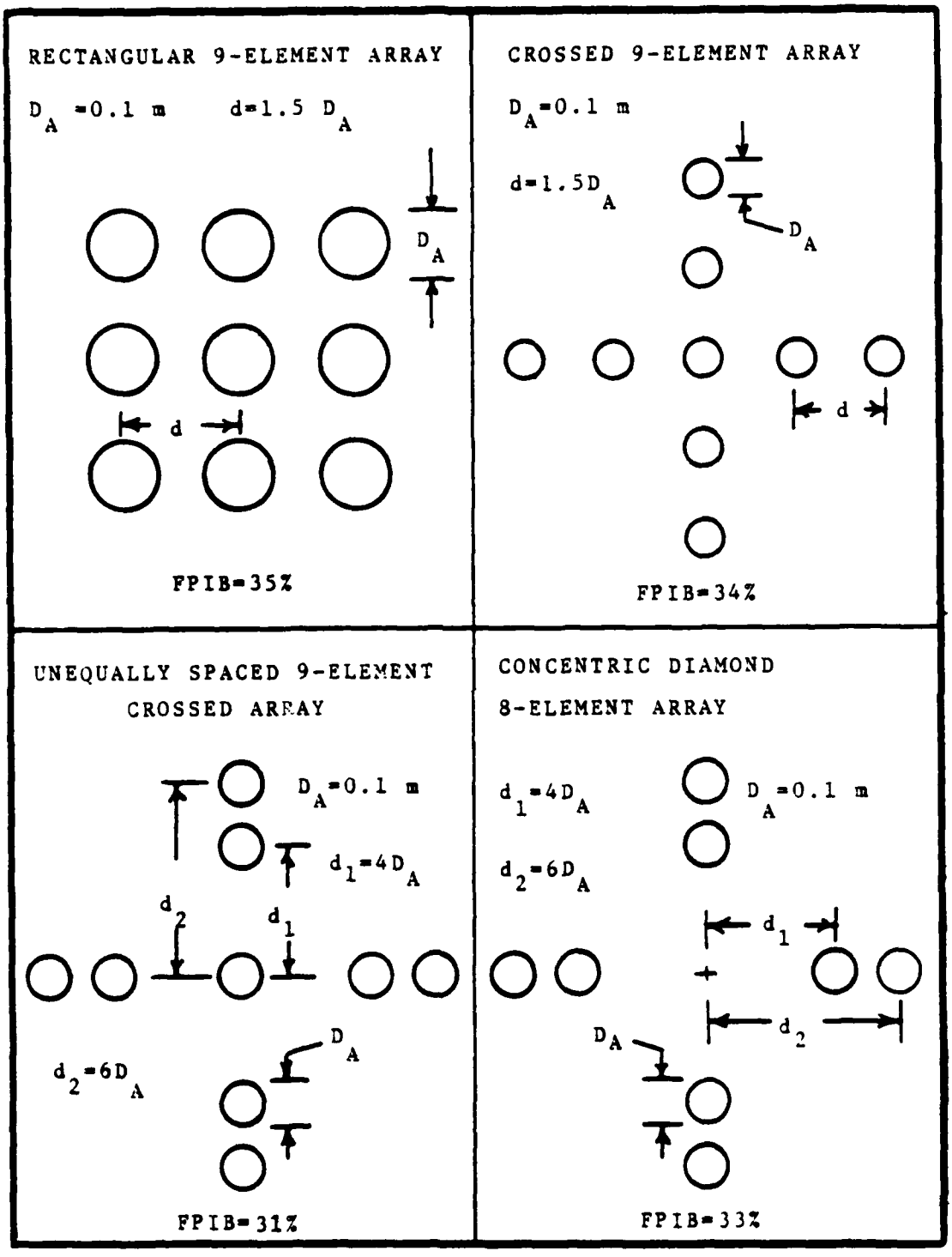

Fig. 3: FPIB FOR VARIOUS ARRAY CONFIGURATIONS

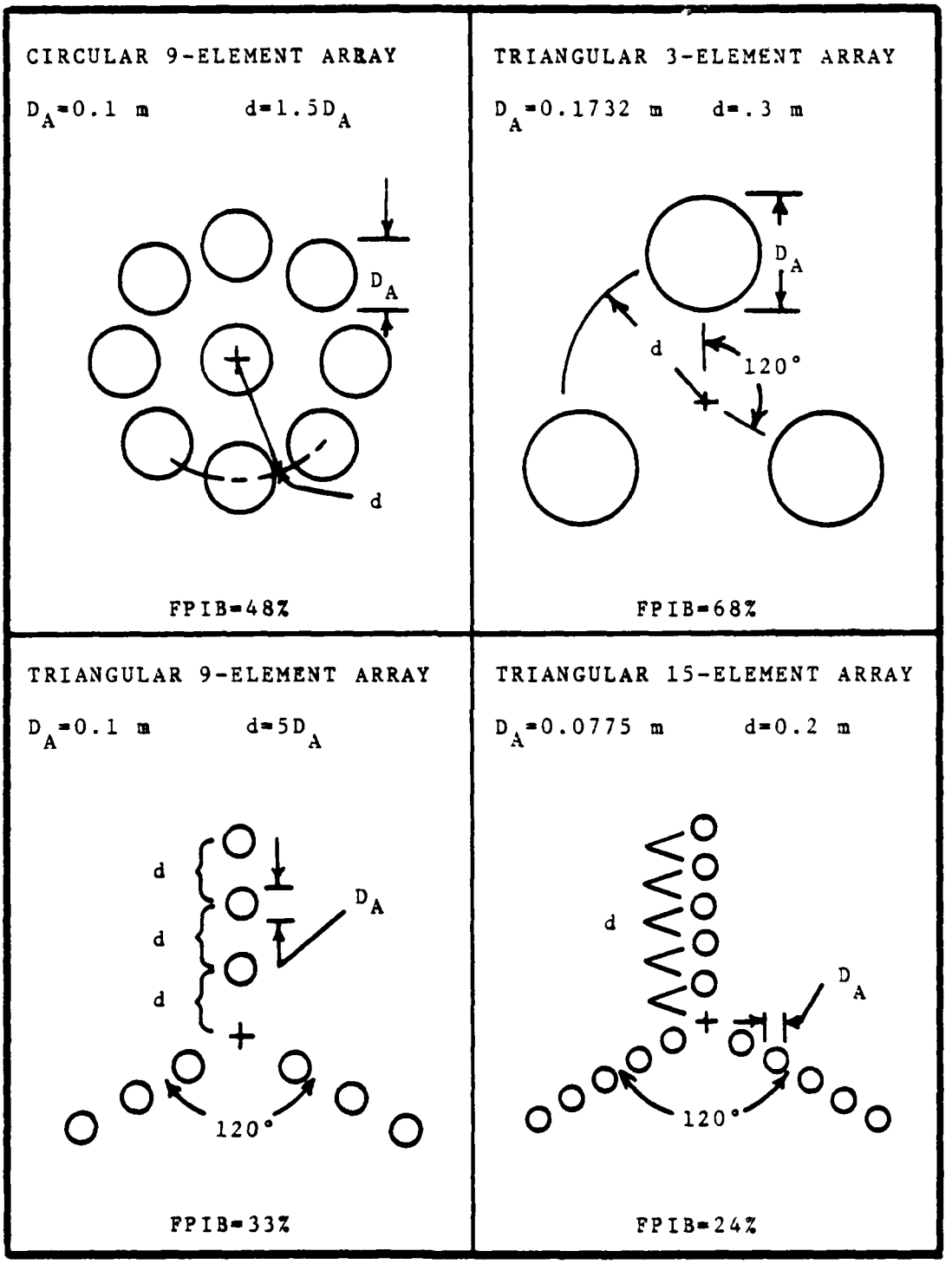

Fig. 3 (continued)

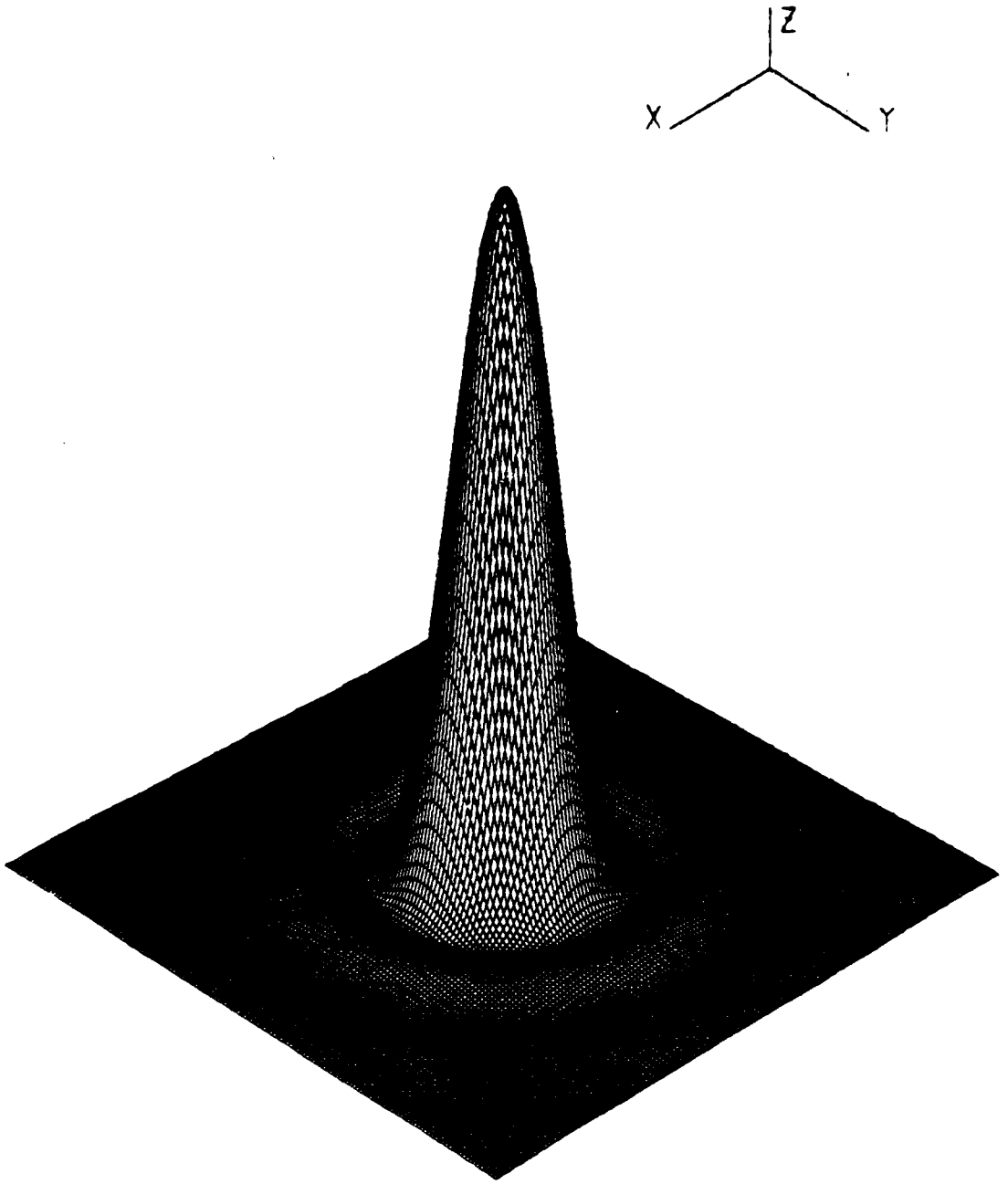

Fig. 4a: IRRADIANCE ON THE TARGET FROM A SINGLE CIRCULAR APERTURE

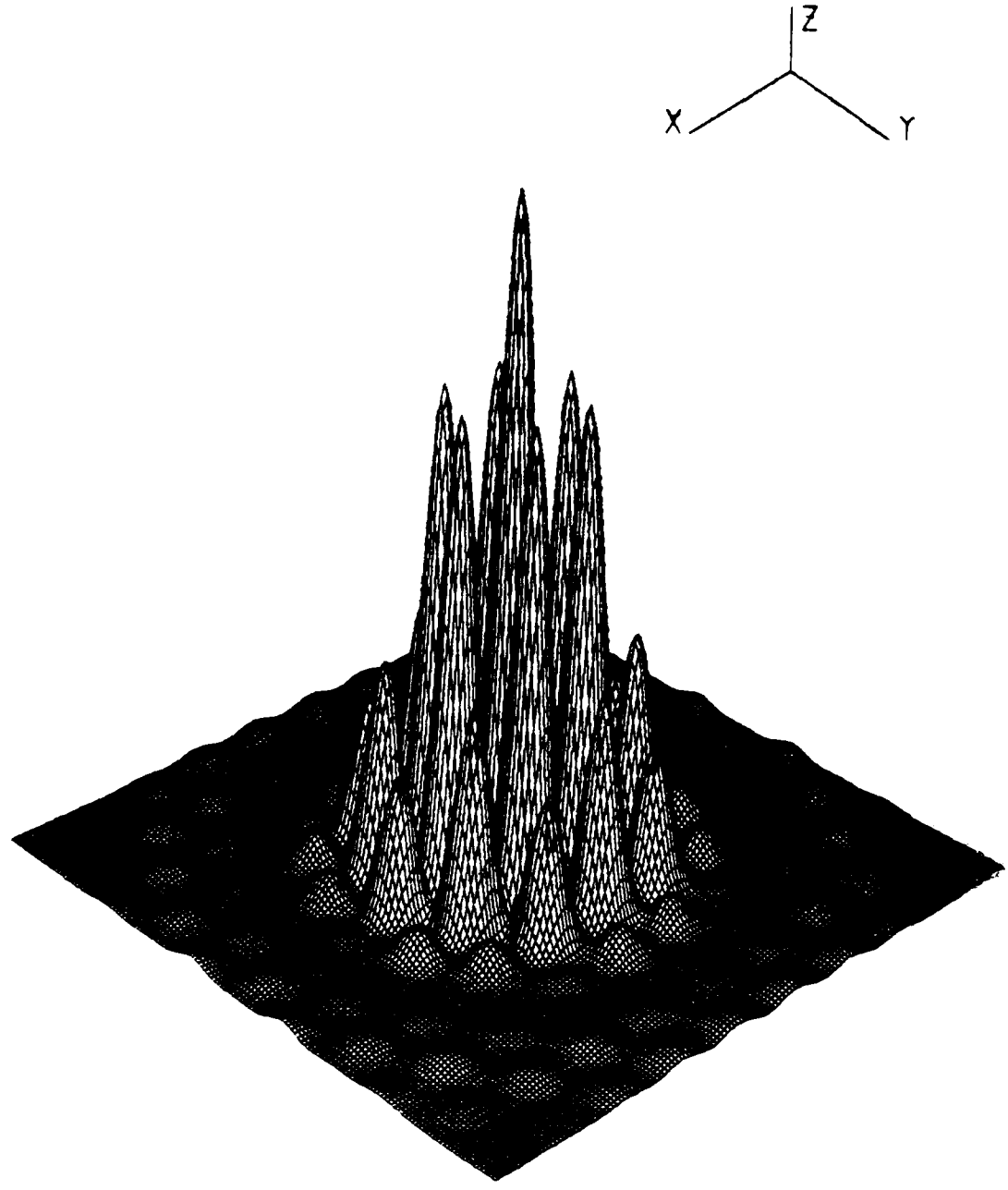

Fig. 4b: IRRADIANCE ON THE TARGET FROM A TRIANGULAR 3-ELEMENT ARRAY

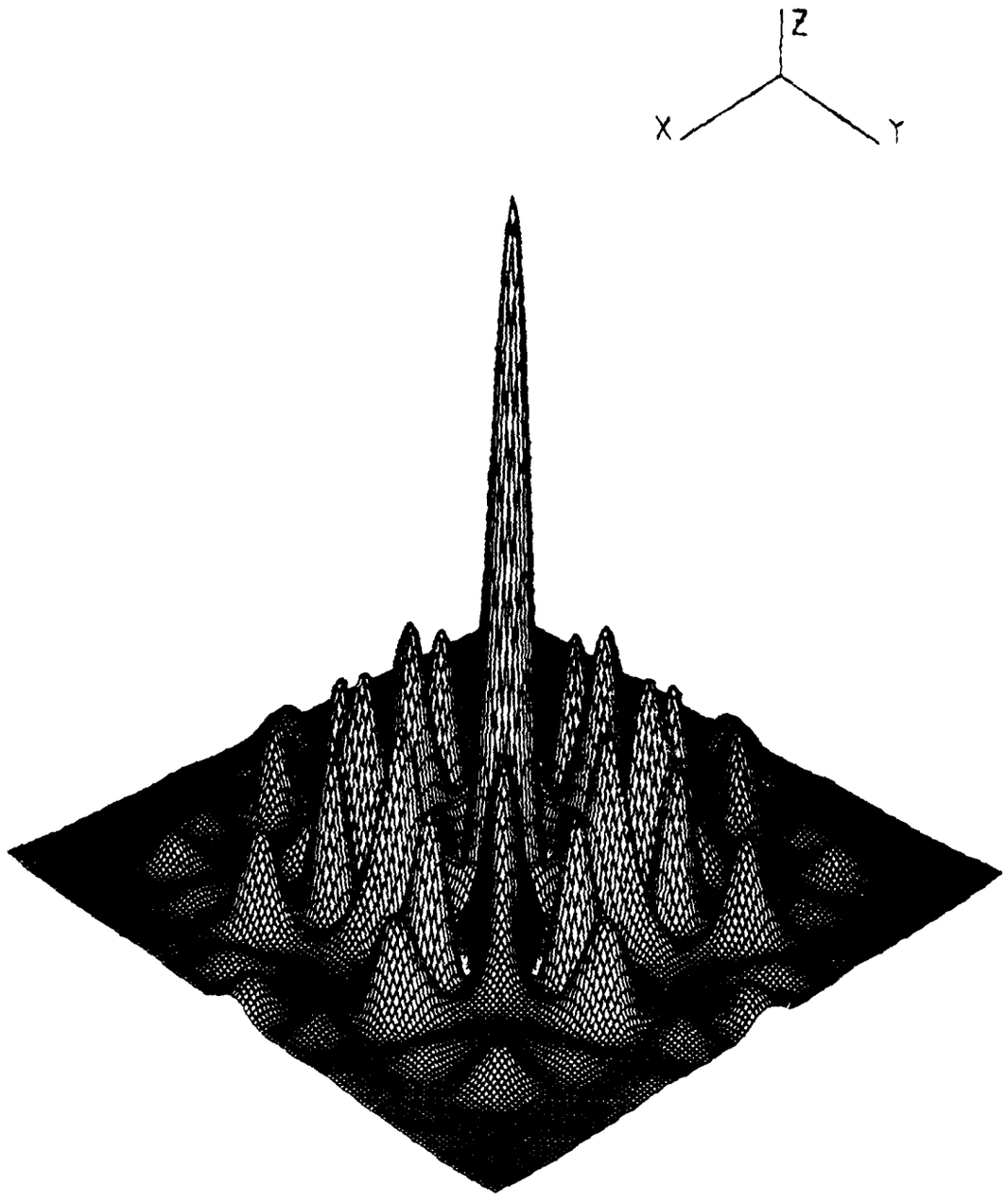

Fig. 4c: IRRADIANCE ON THE TARGET FROM A CIRCULAR 9-ELEMENT ARRAY

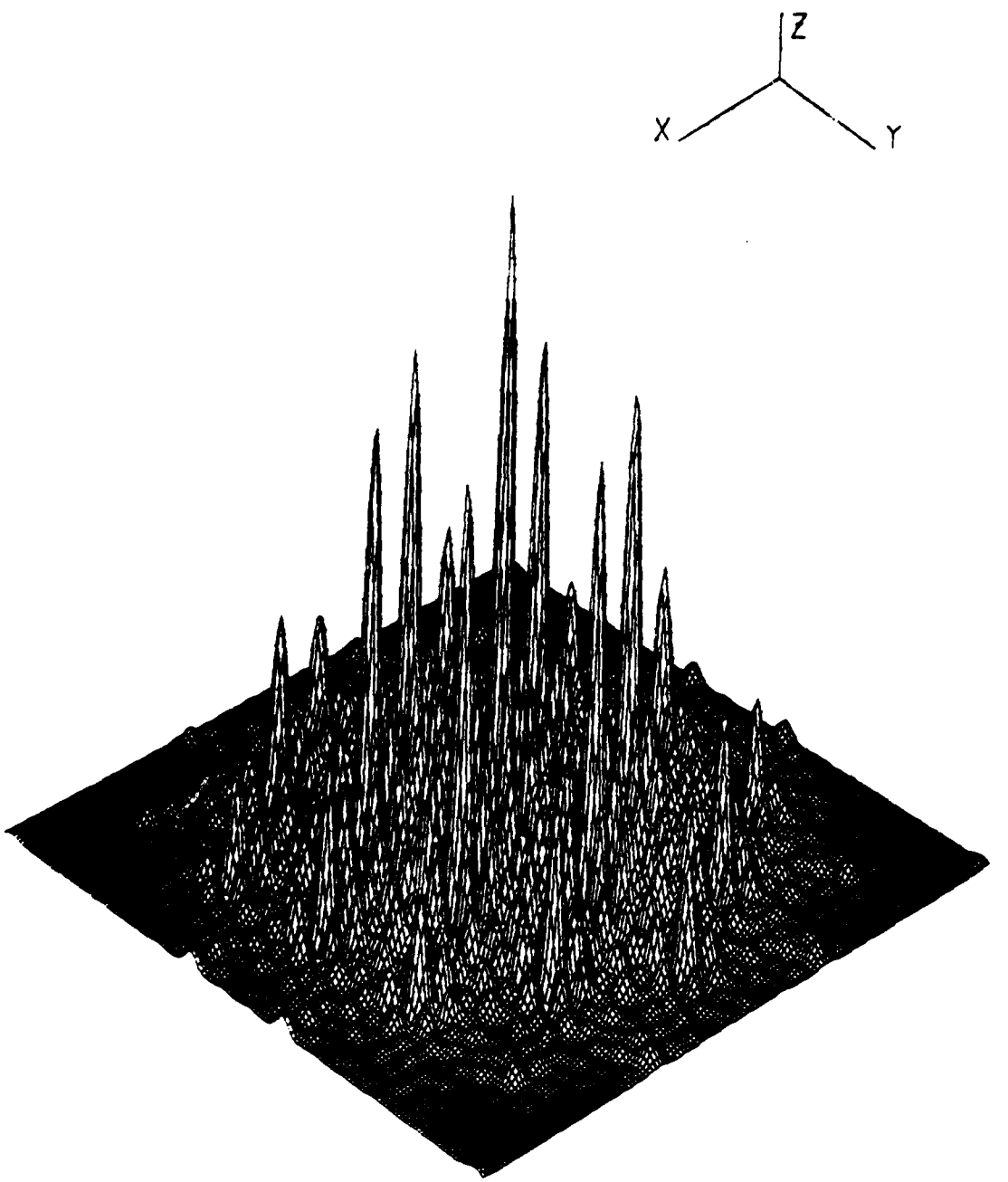

Fig. 4d: IRRADIANCE ON THE TARGET FROM A TRIANGULAR 9-ELEMENT ARRAY

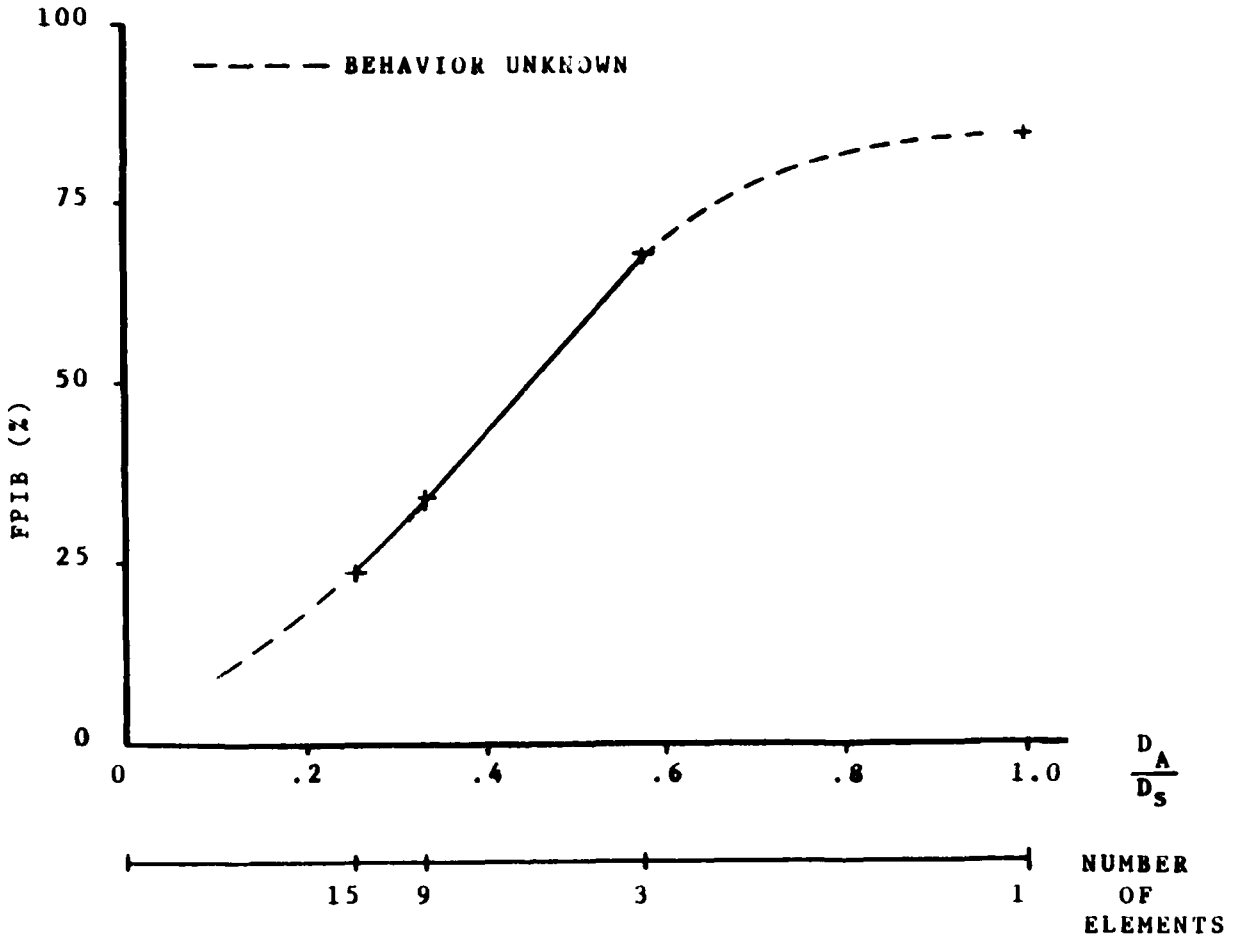

Fig. 5: FPIB VS. ARRAY APERTURE SIZE

IV. FLUID DYNAMICS RELATED TO TURRETS

A. SEPARATED FLOW REGIONS

Behind blunt bodies even at moderate Reynolds numbers turbulent separated flow will occur. Thus, the single large aperture in a circular turret must project through a region of turbulent separated flow such as that shown in Figure 1a.

B. WAKES FROM TURBULENT BOUNDARY LAYERS

Regardless of the body geometry, when the Reynolds number is greater than the critical value, a turbulent wake will be present behind the body. Propagation through a turbulent wake degrades beam quality more than either a separated flow or a turbulent boundary layer.

C. TRANSITION TO TURBULENCE IN THE BOUNDARY LAYER

An array of small scale streamlined turrets can maintain laminar flow over the many smaller turrets if the geometric scale is small enough. An upper bound on the irradiance which mirrors can withstand before distortion and failure requires an equal area in the array as the single aperture to project equal power. The number of array elements then depends on the maximum aperture size that still maintains laminar flow since it is determined that arrays of large apertures achieve greater FPIB than arrays of small apertures.

The array apertures are located inside of aerodynamically streamlined bodies with $X_A/D_A \doteq 6$ * (see Fig. 1d). This design is proposed because of transition at a high Reynolds number, somewhere above $R_c = 2 \times 10^6$ [Ref. 8].

$$V_c = \frac{R_c \nu}{X_A} = \frac{R_c \nu}{6\ D_A} \tag{15}$$

Use of equation (15) and typical values of dynamic viscosity in the atmosphere as a function of altitude [Table 1, Ref. 9] yields a critical velocity below which there is laminar flow over the turret in the array.

TABLE 1

KINEMATIC VISCOSITY VS. ALTITUDE IN THE ATMOSPHERE

height (km)	$\nu \times 10^5$ (m^2/sec)
0	1.4638
1	1.5841
2	1.7171
3	1.8648
4	2.0289
5	2.2119
6	2.4164
7	2.6456
8	2.9032
9	3.1936
10	3.5221
11	3.8948
12	4.5601
13	5.3389
14	6.2508
15	7.3185

*For simplicity in these theoretical analyses it is assumed that the streamlined turret diameter is equal to the aperture (mirror) diameter in Figures 1c and 1d.

For various aperture geometric scales, Figure 6 shows critical velocity at altitudes from sea level to 15 km.

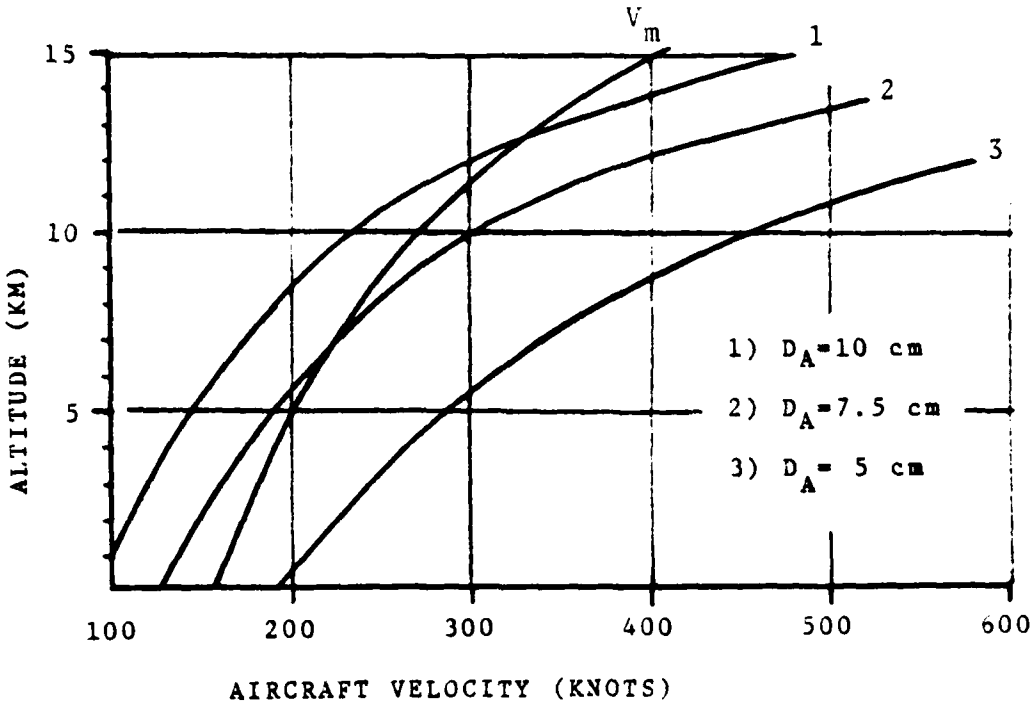

Fig. 6: CRITICAL VELOCITY VS. ALTITUDE

Figures 5 and 6 reveal that aperture geometric scale, the altitude where laminar flow is maintained, and FPIB for the array are all closely linked. It should be noted that an aircraft capable of transporting the laser system may not be able to fly at the velocity which corresponds to certain altitudes and aperture geometric scales. For example, if 35% FPIB is desired from a triangular array, this requires 10-cm apertures in the array if D_s=30 cm. However, at an

altitude of 5 km transition from laminar to turbulent flow occurs at about 145 knots for a 10-cm turret. A large-body jet aircraft probably cannot fly at this speed at an altitude of 5 km.

Thus, an estimate of regions of aircraft operability is needed; recalling the expression for aerodynamic lift:

$$L = \tfrac{1}{2}\rho V^2 S C_L \tag{16}$$

Then

$$V_m = \left[\frac{2L}{\rho S C_L}\right]^{\frac{1}{2}} \tag{17}$$

is the minimum velocity for an aircraft in a no-stall condition. For most large-body jet aircraft L/S is typically about 100 lbs per square foot, and a practical maximum for C_L is assumed to be 1.2. V_m as a function of altitude has been computed and is also shown in Figure 6.

V. INFLUENCE OF TURBULENT BOUNDARY LAYER ON POWER IN THE BUCKET

A. SELECTION OF MODEL

An estimate of PIB for the large single aperture is sought. The literature contains theoretical discussion of beam quality for propagation through turbulent boundary layers of uniform thickness [Ref. 10]. The angular dependence of beam intensity for the SAT is estimated by such a model.

B. ESTIMATION OF PIB FOR SAT

Sutton has calculated the time averaged angular dependence of beam irradiance for several cases of beam diameters (D_s), energy containing turbulence wavelength (a) and boundary layer thickness (L) for the above model.

Data points were taken from Figure 2 of Sutton [Ref. 11] which plots I/I_o vs. $\Theta D_s/\lambda$. The trapezoidal rule was used to numerically integrate

$$PIB_{SAT} = \int_0^{1.22} \frac{I(r)}{I_o} \, 2\pi r \, dr \tag{18}$$

where

$$r = \frac{\Theta D_s}{\lambda} \tag{19}$$

A number representing PIB is obtained for each case of D_s/a and αL.* The PIB obtained in this manner is converted to FPIB by comparison to the result of the above integration using $I(r)/I_o$ for the Airy distribution, which is known.

$$FPIB_{SAT} = \frac{PIB_{SAT}}{PIB_{AIRY}} \cdot 83.8\% \qquad (20)$$

Table 2 shows these results. The program is in Appendix B.

TABLE 2

FPIB FOR SELECTED VALUES OF D_s/a AND αL

D_s/a \ αL	1	2	4	10
1	.799	.812	.776	.570
10	.380	.172	.059	.014
100	.338	.117	.016	.0004

*a is nearly equal to Λ, the turbulence integral scale [Ref. 12]

To find the region of Table 2 which most closely corresponds to the case of the single aperture streamlined turret, the following equations are used to estimate αL and D_s/a. The equation for the extinction coefficient in the turbulent boundary layer is obtained from Sutton [Ref. 13].

$$\alpha = 2k^2 \langle \Delta n^2 \rangle \Lambda \tag{21}$$

where k is the wavenumber, Δn the change in refractive index, and Λ the turbulence integral scale which Sutton [Ref. 14] estimates as

$$\Lambda = 0.1\ L \tag{22}$$

L is the path length through the turbulent boundary layer or the boundary layer thickness. This length is estimated using the equation for the flow of an incompressible fluid in a turbulent boundary layer [Ref. 15] beginning at the front edge of a flat plate.

$$L = 0.37 \left[\frac{\mu X^4}{\rho V} \right]^{0.2} \tag{23}$$

The variables μ and ρ have the usual meanings, V is the aircraft speed, and X is the distance from the leading edge (front of the streamlined body in this case). The beam emerges from the rear of the body at a distance perhaps 4/5 of the body length back from the front, or $5D_s$. A reasonable estimate for L is therefore

$$L = 0.37 \left[\frac{5^4 \mu}{\rho V} \right]^{0.2} D_s^{0.8} \tag{24}$$

Let $C_2 = 0.37 \, (625\mu/\rho V)^{0.2}$, which is clearly dependent on altitude and velocity. Substitution shows that

$$L = C_2 (h,V) \, D_s^{0.8} \tag{25}$$

It is known that

$$\Delta n = K(\rho_\infty) \frac{\Delta\rho}{\rho_\infty} \tag{26}$$

or

$$\Delta n = K_{SL} \, e^{-h/H} \frac{\Delta\rho}{\rho_\infty} \tag{27}$$

where K is the constant in the equation relating refractive index to density, i.e., $n=1 + K\rho/\rho_\infty$, H is the scale height, $\Delta\rho$ is the change in local density, and ρ_∞ is the ambient air density. From Sutton [Ref. 16] one obtains the relation for the last term in Equation (27).

$$\frac{\Delta\rho}{\rho_\infty} = 0.1 \left(1 - \frac{\rho_W}{\rho_\infty} \right) \tag{28}$$

where ρ_W is the density of air on the surface of the turret. Assuming an ideal gas and constant pressure across the boundary layer

$$\frac{\Delta\rho}{\rho_\infty} = 0.1 \left(1 - \frac{T_W}{T_\infty} \right) \tag{29}$$

Liepmann and Roshko [Ref. 17] provide an expression for the stagnation temperature ($T_o = T_w$) as a function of the ambient temperature (T_∞), M the Mach number, and γ the ratio of heat capacities.

$$T_w = T_\infty \left(1 + \frac{\gamma-1}{2} M^2\right) \tag{30}$$

Since stagnation temperature is equated to wall temperature, Equation (30) is valid only for Prandtl number of unity. From the above equations it can now be shown that

$$\alpha L = 2\left(\frac{2\pi}{\lambda}\right)^2 10^{-3} K_{SL}\, e^{-2h/H} \left[\frac{\frac{\gamma-1}{2} M^2}{1+\frac{\gamma-1}{2} M^2}\right] C_2^2\, D_S^{1.6} \tag{31}$$

Typical values for substitution into (31) are H = 7.6 km, h = 5 km, D_S = 0.3m, γ = 1.4, $K_{SL} = 5\times10^{-4}$, M = 0.3, and C_2(5 km, 250 knts) = 0.16 $m^{0.2}$. These values produce an extinction number (αL) of about 1.1×10^{-3}. From Figure 2 of Sutton [Ref. 18] it is evident that the beam is negligibly affected by the turbulent boundary layer and therefore very close to the diffraction-limited case regardless of the ratio D_S/a.

VI. CONCLUSIONS

Laser turrets designed with today's technology may be ineffective against an airborne target aft of the aircraft. An array of apertures using a future technology window and proper phase retardation can achieve reasonable Fractional Power in the Bucket (FPIB) on a target approaching an aircraft from behind. This FPIB is largely dependent on the aperture diameter of the array elements and is relatively insensitive to interaperture spacing as long as the Fraunhofer condition is satisfied.

However, possession of the technology for a small scale window (see Fig. 1d) for use in the array would probably also yield the technology for the large window (see Fig. 1c) soon thereafter. Given the flexibility of both large and small window technologies, the single turret shown in Figure 1c is by far the better.

Even though the array achieves laminar flow and small windows may be easier to develop, such a system incurs the price of a collosal fire control problem, phase control problem, and the operational restriction of flight velocities near the aircraft stall speed. Surprisingly, the single turret design is negligibly affected by the turbulent boundary layer and therefore nearly diffraction limited upon exit from the boundary layer. Though it does create a wake which is

turbulent, reasonable advance detection of targets approaching from behind should avoid the necessity to try to project directly aft through the wake.

APPENDIX A

PROGRAM LISTING
GRID SUMMATION

```
C THIS PROGRAM COMPUTES THE IRRADIANCES IN THE TARGET PLANE AND SUMS
C THESE IRRADIANCES TO FIND THE PIB FOR A CIRCULAR 9-ELEMENT ARRAY
      REAL R20,RHO,AX(9),AY(9),TX,TY,DEL(9),A,D,H,K,ENV(401,401)
      REAL ALFA,BETA,ARGBES,RES,EPS,RAD
      REAL ABCSSA(401),ITNS(401),LAMBDA,TTNS(401),RHOTAR
      REAL*8 POWER
      INTEGER I,J,II,JJ,N,IER
          N=1
          EPS=.00001
          A=.1
          D=.15
          H=5.0
          RAD=4.065566303
          LAMBDA=1E-05
          K=2.0*3.141592654/LAMBDA
          R20=100000.
          AA=SQRT(2.0)
          POWER=0.0
          AX(1)=D/AA
          AX(2)=0.
          AX(3)=-D/AA
          AX(4)=D
          AX(5)=0.
          AX(6)=-D
          AX(7)=D/AA
          AX(8)=0.
          AX(9)=-D/AA
          AY(1)=D/AA
          AY(2)=D
          AY(3)=D/AA
          AY(4)=0.
          AY(5)=0.
          AY(6)=0.
          AY(7)=-D/AA
          AY(8)=-D
          AY(9)=-D/AA
      JJ=0
      DO 30 J=1,400
          DO 20 I=1,400
              ABCSSA(I)=H*(FLOAT(I-1))/400.0
```

```
            TX=H*(FLOAT(I-1))/400.
            TY=H*(FLOAT(J-1))/400.
            ALFA=0.0
            BETA=0.0
            DO 10 II=1,9
               RHO=SQRT(AX(II)**2+AY(II)**2)
               DEL(II)=((RHO**2)/2.-AX(II)*TX-AY(II)*TY)/R20
               ALFA=COS(K*DEL(II))+ALFA
               BETA=SIN(K*DEL(II))+BETA
 10         CONTINUE
            ARGBES=SQRT(TX**2+TY**2)*A*3.1415926254/(R20*LAMBDA)
            CALL BESJ(ARGBES,N,RES,EPS,IER)
            IF((I.EQ.1).AND.(J.EQ.1))ARGBES=1.
            ENV(J,I)=(2.*RES)/ARGBES
            IF((I.EQ.1).AND.(J.EQ.1))ENV(J,I)=1.
            ENV(J,I)=(ALFA**2+BETA**2)*ENV(J,I)**2
            IF(J.EQ.I)ITNS(I)=ENV(J,I)
            IF(J.EQ.I)TTNS(I)=(ALFA**2+BETA**2)
            RHOTAR=SQRT(TX**2+TY**2)
            IF(RAD.LT.RHOTAR)GOTO19
               IF(.NOT.((J.EQ.1).AND.(I.EQ.1)))GOTO17
                  ENV(J,I)=ENV(J,I)*.25
                  GOTO18
 17            CONTINUE
               IF(.NOT.((J.EQ.1).OR.(I.EQ.1)))GOTO18
                  ENV(J,I)=ENV(J,I)*.50
 18            CONTINUE
               POWER=POWER+ENV(J,I)
               JJ=JJ+1
 19         CONTINUE
    IF(I.EQ.J)WRITE(6,300)ARGBES,RES,ITNS(J),TTNS(J),POWER,ABCSSA(J)
 20      CONTINUE
 30 CONTINUE
    WRITE(6,50)POWER,JJ
    WRITE(6,100)
    CALL PLOTP(ABCSSA,ITNS,400,0)
    WRITE(6,100)
    CALL PLOTP(ABCSSA,TTNS,400,0)
 50 FORMAT(//1X,F13.4,5X,I8)
100 FORMAT('1')
200 FORMAT(5(3X,F8.6))
300 FORMAT(1X,6(1X,F10.2),2X)
400 FORMAT(1X,I2)
    STOP
    END
```

APPENDIX B

PROGRAM LISTING
TRAPEZOIDAL RULE

```
C THIS PROGRAM COMPUTES THE VOLUME UNDER ANY SET OF DATA POINTS THAT
C HAVE BEEN ROTATED AROUND THE FIRST, AS WELL AS THE
C VOLUME UNDER THE AIRY DISK...INPUT A TITLE _ RETURN _ INPUT 7 VALUES
      REAL H,Y(7),Z(7),X(7),BJ,D,U(7),TITLE(5)
      INTEGER NDIM,IER
      NDIM=7
      READ(5,400)(TITLE(I),I=1,5)
      READ(5,100)(X(I),I=1,7)
      WRITE(6,800)
      WRITE(6,500)(TITLE(I),I=1,5)
      WRITE(6,300)
      PI=3.141592654
      N=1
      H=.2
      D=.00001
      DO 10 I=1,7
         Y(I)=X(I)*2.*H*FLOAT(I-1)*PI
   10 CONTINUE
      CALL QSF(H,Y,Z,NDIM)
      DO 12 I=1,7
         WRITE(6,200)I,X(I),Y(I),Z(I)
   12 CONTINUE
      WRITE(6,300)
      WRITE(6,300)
      DO 20 I=1,7
         X(I)=H*FLOAT(I-1)*PI
         CALL BESJ(X(I),N,BJ,D,IER)
         Y(I)=0.0
         IF(I.EQ.1)GOTO15
            U(I)=((2.*BJ/X(I))**2)
            Y(I)=2.*PI*H*FLOAT(I-1)*U(I)
   15    CONTINUE
         WRITE(6,600)I,X(I),BJ,Y(I),U(I)
   20 CONTINUE
      CALL QSF(H,Y,Z,NDIM)
      WRITE(6,300)
      WRITE(6,700)(Z(I),I=1,7)
      WRITE(6,800)
  100 FORMAT(7F5.2)
  200 FORMAT(1X,I3,3X,3(3X,F10.7))
```

```
300 FORMAT(///)
400 FORMAT(5A4)
500 FORMAT(1X,5A4)
600 FORMAT(1X,I3,3X,4(3X,F10.7))
700 FORMAT(1X,'AIRY DISK INTEGRAL VALUES',3(3X,F10.7))
800 FORMAT('1')
    STOP
    END
```

LIST OF REFERENCES

1. Born, M. and Wolfe E., Principals of Optics, Pergamon Press, 1964.

2. Stone, J. M., Radiation and Optics, Figure 7-4, pp. 118, McGraw-Hill, 1963.

3. Ibid., pp. 120-121.

4. Isaacman, R., "Using Earth as a Radio Telescope; Very Large Array," Astronomy, Vol. 7., pp. 6-13, October 1979.

5. Thomsen, D. E., "VLA Field Day," Science News, Vol. 119, No. 8, pp. 122-3, 21 February 1981.

6. Wigglesworth, V. B., "Insect Vision' , The Life of Insects, Weidenfeld and Nicolson, 1964.

7. Lockwood, A. P. M., "Sense Organs", Physiology of Crustacea, W. H. Freeman and Company, 1967.

8. Hoerner, S. F., Fluid-Dynamic Drag, Hoerner Fluid Dyanmics, 1965.

9. National Advisory Committee for Aeronautics Report 1235, Standard Atmosphere - Tables and Data for Altitudes to 65,800 Feet, 1955.

10. Sutton, G. W., "Effect of Turbulent Fluctuations in an Optically Active Fluid Medium," AIAA Journal, Vol. 7, No. 9, September 1969.

11. Ibid., pp. 1741.

12. Ibid., Equation (14).

13. Ibid., Equation (37).

14. Sutton, G. W., On Optical Imaging Through Aircraft Turbulent Boundary Layers, from proceedings of the Aero-Optics Symposium on Electromagnetic Wave Propagation from Aircraft, NASA-Ames Research Center, Moffett Field, CA., pp. 241, 14-15 August 1979.

15. Dwinnel, J. H., Principles of Aerodynamics, McGraw-Hill, 1949, pp. 157.

16. Sutton, On Optical Imaging Through Aircraft Turbulent Boundary Layers, Equation (14).

17. Liepmann, H. W. and Roshko, A. Elements of Gasdynamics, John Wiley and Sons, 1957.

18. Sutton, G. W., "Effect of Turbulent Fluctuations in an Optically Active Fluid Medium."

INITIAL DISTRIBUTION LIST

		No. of Copies
1.	Defense Technical Information Center Cameron Station Alexandria, Virginia 22314	2
2.	Library, Code 0142 Naval Postgraduate School Monterey, California 93940	2
3.	Department Chairman, Code 67 Department of Aeronautics Naval Postgraduate School Monterey, California 93940	1
4.	Distinguished Professor A. E. Fuhs Code 67Fu Department of Aeronautics Naval Postgraduate School Monterey, California 93940	10
5.	Professor Edmund A. Milne Code 61Mn Department of Physics Naval Postgraduate School Monterey, California 93940	1
6.	Department Chairman, Code 61 Department of Physics and Chemistry Naval Postgraduate School Monterey, California 93940	1
7.	Commandant (G-PTE-1/TP-41) USCG Headquarters Washington, DC 20593	2
8.	Lieutenant Brian B. Tousley 715 Kieffer Street Wooster, Ohio 44691	2

9. Captain Richard de Jonckheere, USAF — 5
AFWL/ARLB
Kirtland AFB, N.M. 87117

10. Professor A. W. Cooper — 1
Code 61Cr
Department of Physics
Naval Postgraduate School
Monterey, California 93940


FILMED
8